

Interactions between the Exocytic and Endocytic Pathways in Polarized Madin-Darby Canine Kidney Cells*

Received for publication, December 20, 1999, and in revised form, February 14, 2000

Ena Orzech[‡], Shulamit Cohen[‡], Aryeh Weiss[§], and Benjamin Aroeti^{‡¶}

From the [‡]Department of Cell and Animal Biology, Institute of Life Sciences, Hebrew University of Jerusalem, Jerusalem 91904 and the [§]Department of Electronics, Jerusalem College of Technology, Jerusalem 91160, Israel

The compartments involved in polarized exocytosis of membrane proteins are not well defined. In this study we hypothesized that newly synthesized polymeric immunoglobulin receptors are targeted from the *trans*-Golgi network to endosomes prior to their appearance on the basolateral cell surface of polarized Madin-Darby canine kidney cells. To examine this hypothesis, we have used an assay designed to measure the meeting of newly synthesized receptors with a selective population of apical or basolateral endosomes loaded with horseradish peroxidase. We found that in the course of basolateral exocytosis, the wild-type polymeric immunoglobulin receptor is targeted from the *trans*-Golgi network to apical and basolateral endosomes. Phosphorylation of a Ser residue in the cytoplasmic tail of the receptor is implicated in this process. The biosynthetic pathway of apically sorted polymeric immunoglobulin receptor mutants similarly traversed apical endosomes, raising the possibility that apical receptors are segregated from basolateral receptors in apical endosomes. The post-endocytic pathway of transcytosing and recycling receptors also passed through apical endosomes. Together, these observations are consistent with the possibility that the biosynthetic and endocytic routes merge into endosomes and justify a model suggesting that endosomal recycling processes govern polarized trafficking of proteins traveling in both pathways.

Epithelial cells carry out a variety of vectorial transport and secretory processes that profoundly depend upon the polarized distribution of proteins and lipids on their cell surface. The plasma membrane of epithelial cells can generally be divided into two domains, an apical surface that faces the external environment and a basolateral surface contacting adjacent cells and underlying tissues. The two surface domains display a completely different protein and lipid composition. The precise intracellular compartment(s) in which proteins destined for the apical and basolateral cell surface are sorted is not certain. It is commonly believed that the combined ability of endosomes and the *trans*-Golgi network (TGN)¹ to target a

membrane protein to a particular surface domain plays a role in determining its polarized steady-state distribution on the plasma membrane (1–4).

The TGN is thought to serve as a major sorting site for plasma membrane proteins traveling in the biosynthetic pathway (1, 5). This notion is based primarily on observations of a common intracellular localization of apical and basolateral proteins throughout the Golgi stacks (6) and the TGN (7). However, these data do not rule out the possibility that sorting of newly synthesized proteins can take place at later compartments, for instance, in endosomes (1, 2, 4, 8). In this case, membrane proteins would be delivered directly from the TGN to endosomes prior to their appearance on the cell surface. Results from recent studies in nonpolarized cells are consistent with this notion (9, 10). For example, Futter *et al.* (10) showed that the transferrin receptor (TfnR) is targeted first from the TGN to endosomes and is subsequently delivered to the plasma membrane. More recently, Brachet *et al.* (11) have suggested that the biosynthetic pathway of MHC class II molecules traverses early endosomes and that the passage through the endocytic compartment is required to gain access to peptide-loading compartments. In contrast, the biosynthetic pathway of other membrane proteins, such as glycosylphosphatidylinositol-linked proteins, seem to bypass endosomes (10). Hence, diverse pathways (mechanisms) can direct membrane proteins from the TGN to the plasma membrane in nonpolarized cells. Whether similar direct and indirect pathways exist in polarized cells is currently unknown.

Here we analyzed the polarized exocytic transport of the polymeric immunoglobulin receptor (pIgR) exogenously expressed in polarized Madin-Darby canine kidney (MDCK) cells (12). The current model suggests that the pIgR is synthesized in the endoplasmic reticulum, from where it is targeted to the Golgi complex. From the TGN the pIgR is directed to the basolateral surface, where it can bind polymeric immunoglobulins, such as dimeric IgA (dIgA) or IgM, and internalize via clathrin-mediated endocytosis into endosomes. The pIgR bound to its ligand then transcytoses from the basolateral to the apical pole of the cell. The process of pIgR transcytosis utilizes several endosomal compartments, each of which is presumed to play a role in its trafficking to the apical plasma membrane. Initially, upon internalization from the basolateral plasma membrane, dIgA-pIgR complexes reach basolateral early (sorting) endosomes (BEE). BEE serve as the first station for many other endocytic ligands internalized from the basolateral surface (*e.g.* Tfn, low density lipoprotein, and epidermal growth factor bound to their receptors (13)). These ligands exist at high concentrations in BEE (see Ref. 14). Next, pIgR-dIgA com-

* This work was supported by a grant from the Israel Science Foundation funded by the Israel Academy of Sciences. The costs of publication of this article were defrayed in part by the payment of page charges. This article must therefore be hereby marked "advertisement" in accordance with 18 U.S.C. Section 1734 solely to indicate this fact.

¶ To whom correspondence should be addressed. Fax: 972-2-5617918; E-mail: aroeti@cc.huji.ac.il.

¹ The abbreviations used are: TGN, *trans*-Golgi network; pIgR, polymeric immunoglobulin receptor; BEE, basolateral early endosomes; AEE, apical early endosomes; ARE, apical recycling endosomal compartment; CE, common endosomal compartment; SC, secretory component; MDCK, Madin-Darby canine kidney; dIgA, dimeric IgA; CKII, casein kinase II; BFA, brefeldin A; MPR, mannose-6-phosphate receptor; WGA, wheat-germ agglutinin; Tfn, transferrin; TfnR, Tfn receptor;

hTfnR, human tfnR; DAB, diaminobenzidine; FITC, fluorescein isothiocyanate; HRP, horseradish peroxidase; MEM, minimal essential medium; BSA, bovine serum albumin; TDB, Triton dilution buffer; PAGE, polyacrylamide gel electrophoresis.

plexes are transported to a compartment that consists of long, 60-nm diameter tubules lying parallel to microtubules and oriented toward the apical cytoplasm (15). The "tubular compartment" contains both IgA and transferrin at the same relative concentrations as the BEE but is substantially depleted of low density lipoprotein and epidermal growth factor receptor, which are destined for the degradative pathway (13, 14). This compartment, which resides in the medial and apical cytoplasm of polarized MDCK and Caco-2 cells, has been designated the "interconnected compartment" or the "common endosomal compartment" (CE) (14–18). The final compartment in the transcytotic pathway is comprised of 100–150-nm cup-shaped vesicles distributed underneath the apical plasma membrane (13). This compartment is likely the equivalent of the pericentriolar apical recycling endosomal compartment (ARE), whose structure depends upon microtubules (19, 20).

Electron microscopic and quantitative immunofluorescence localization data suggest that ARE are enriched in the transcytotic marker, the pIgR, but are relatively depleted in the recycling marker, the human TfnR (hTfnR) (13, 14). The endosomal rabs, rab11a, rab17, and rab25 are associated with this compartment (21, 22). Fluid phase ligands internalized from the apical plasma membrane reach apical early endosomes (AEE) but not ARE or the CE (19). ARE and CE, however, can be reached by membrane-bound endocytic ligands such as dIgA, Tfn, or the general endocytic tracer ricin (13, 20, 23), suggesting that CE, ARE, and AEE are distinct compartments. Apical endosomes have become the focus of intense interest, because they appear to serve as a major intersection site for various post-endocytic (transcytotic and recycling) receptors in epithelia. On the basis of these and other observations it has been postulated that in epithelial cells, apical and basolateral sorting as well as recycling of endocytic receptors is mediated by CE and/or in ARE (21, 24).

A significant level of pIgR transcytosis can also occur when the pIgR is not bound to its ligand. This process has been referred to as constitutive transcytosis (25), whose presumptive trigger is phosphorylation of a cytoplasmic Ser, Ser⁶⁶⁴ (26, 27). Like ligand-bound pIgR, the unoccupied pIgR also reaches ARE *en route* to the apical cell surface (19). Thus, both dIgA-mediated and constitutive transcytosis of the pIgR are potentially regulated by multiple endosomal compartments.

The 17-residue cytoplasmic segment positioned immediately after the transmembrane domain of the pIgR has been characterized as an autonomous and dominant basolateral sorting signal (28). An in-frame deletion of fourteen amino acids in this segment results in sorting of the pIgR from the TGN to the apical plasma membrane. Individual residues (His⁶⁵⁶, Arg⁶⁵⁷, and Val⁶⁶⁰) within the 17-residue peptide have been shown to be important for mediating basolateral transport of the receptor (29, 30). However, a fraction of the pIgR mutants impaired in basolateral sorting can reach the basolateral surface, internalize into basolateral endosomes, and transcytose to the apical surface. Intriguingly, the mutant receptors displayed enhanced transcytotic activity (8). Hence, mutations that inhibited basolateral targeting and increased apical targeting from the TGN similarly decreased basolateral recycling from endosomes and increased basolateral-to-apical transcytosis. Mutations in the basolateral targeting signal of the low density lipoprotein receptor that affect the polarity of biosynthetic sorting show similar enhancement of its apical sorting after endocytosis (31). One interpretation of these observations is that the targeting signal acts in two different locations: in the TGN during exocytosis and in endosomes after endocytosis. This suggests that a similar type of sorting machinery operates in both the TGN and endosomes. An alternative model argues

that the constitutive exocytic and post-endocytic pathways of the pIgR converge into a common sorting compartment. This compartment is unlikely to be the TGN (8, 31) but may be endosomes. The latter model would predict the direct targeting of newly synthesized pIgR from the TGN to endosomes.

A casein kinase II (CKII) phosphorylation motif in the cytoplasmic tail of the mannose-6-phosphate receptor (MPR) is thought to mediate MPR interaction with the Golgi-associated clathrin AP-1 adaptor (32, 33). A number of observations argue that AP-1 binding may be coupled to the subsequent process of MPR budding into clathrin-coated vesicles and transport from the TGN to endosomes (34–36). We have recently suggested that phosphorylated Ser⁷²⁶ residing in a putative CKII/protein kinase A phosphorylation site in the cytoplasmic tail of pIgR mediates the association of AP-1 adaptor with the pIgR (37). These observations further suggested to us that similar to MPR, AP-1 association with phosphorylated Ser in the cytoplasmic tail of pIgR elicits the sequestration of pIgR into clathrin-AP-1-coated domains in the TGN, from where it could be transported to endosomes, prior to its appearance on the basolateral cell surface. In the present study we took morphological and biochemical approaches to assess this hypothesis and found that the polarized exocytic pathway taken by the pIgR may involve various endosomal compartments.

EXPERIMENTAL PROCEDURES

Proteins and Antibodies

Lectin-triticum vulgaris (wheat germ agglutinin (WGA)) coupled to horseradish peroxidase (HRP) and free HRP Type II were from Sigma. Human apo-transferrin (hTfn; Biological Industries Co, Beit hemeek, Israel) was loaded with iron as described (38). Rabbit antiserum directed against a peptide in the cytoplasmic domain of the rat TGN resident protein, TGN-38 (39), was kindly provided by Dr. G. Banting (University of Bristol, Bristol, UK) and was used at 1:500 and 1:100 dilution for Western blotting and immunofluorescence, respectively. Fab fragments derived from affinity purified guinea pig anti-rabbit SC polyclonal antibodies were a kind gift from Prof. K. Mostov (University of California, San Francisco) and were prepared as described previously (40). Radioiodination of Fabs was performed according to the iodine monochloride protocol (40).

Cell Lines

MDCK cell lines that exogenously co-express the wild-type pIgR and hTfnR was established as described (14). We have used MDCK cells expressing various pIgR constructs. Some of their basic characteristics are summarized in Fig. 1. To obtain cells with higher expression levels, the pIgR-ΔR655-Y668 mutant was re-expressed in MDCK cells using the pCB6 vector (41), as described (29). The pIgR mutant, pIgR-S726-t, whose 30 C-terminal amino acids have been deleted was described and characterized in an earlier work (designated 725t in Ref. 42; see also Fig. 1). This pIgR mutant also exhibited low expression levels and was therefore re-expressed in MDCK cells. In both cases, cell lines exhibiting pIgR expression levels comparable with those of other pIgR-WT expressing cell lines were isolated. Exocytic and endocytic trafficking characteristics of the re-expressed mutant receptors were identical to those described for the original expressors. All MDCK cells were routinely cultured on 10-cm dishes, in minimal essential medium (MEM; Sigma) containing 5% fetal bovine serum and 1% antibiotics (Biological industries, Beit Haemek, Israel). Cells were maintained in culture up to 10 passages. To induce polarity, cells were cultured on 12-mm Transwell filters (Costar) for at least 4 days prior to each experiment. Cell polarity was estimated by measuring gp80 secretion as described (29).

The Diaminobenzidine (DAB) Density Shift Meeting Assay

This assay is designed to measure the meeting of newly synthesized receptors in the exocytic pathway or receptors traveling in the post-endocytic pathway with a selective population of apical or basolateral endosomes loaded with horseradish peroxidase (HRP).

Targeting of Newly Synthesized Receptors to Apical or Basolateral Endosomes—A modified version of the original DAB density shift assay (43) used by Apodaca *et al.* (19) has been applied here to assay the targeting of newly synthesized pIgR to apical or basolateral endosomes. The various steps of the assay are schematically depicted in Fig. 3A.

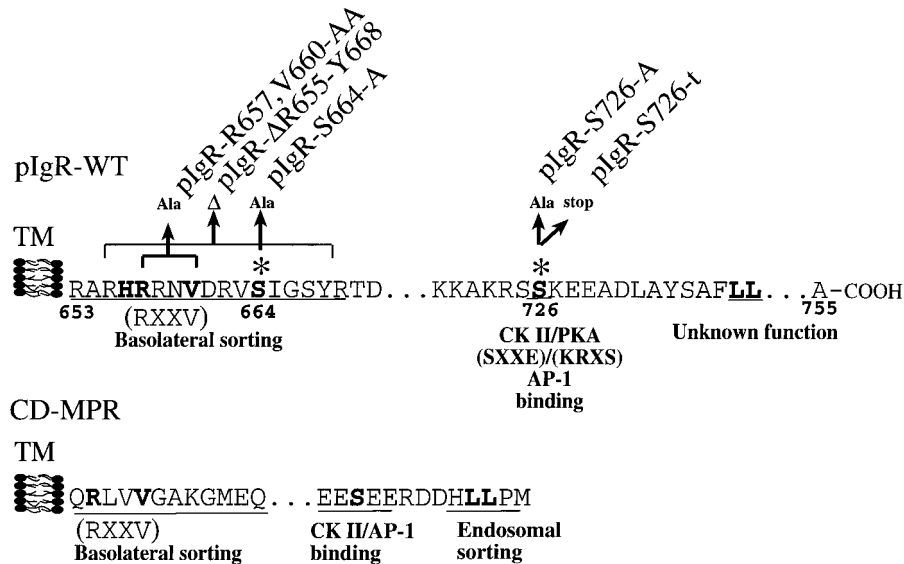


FIG. 1. Schematic presentation of cytoplasmic sorting signals in the pIgR and cation-dependent MPR and mutations constructed by site-directed mutagenesis. *pIgR-WT*, the autonomous 17-residue basolateral sorting signal proximal to the transmembrane domain (TM) is indicated with *underlining*. *pIgR* whose Arg⁶⁵⁷ and Val⁶⁶⁰ have been doubly mutated to Ala (*pIgR-R657,V660-AA*), and *pIgR* whose Arg⁶⁵⁵-Tyr⁶⁶⁸ segment has been deleted in-frame (*pIgR-ΔR655-Y668*) are sorted to the apical cell surface of MDCK cells. Individual amino acids (His⁶⁵⁶, Arg⁶⁵⁷, and Val⁶⁶⁰) that play a role in basolateral sorting of the *pIgR* are marked with *bold letters*. The putative RXXV basolateral sorting motif is indicated in *parentheses*. The two main phosphorylation sites in the cytoplasmic tail (marked with *asterisks*, postulated to be involved in constitutive transcytosis and endocytosis, are Ser⁶⁶⁴ and Ser⁷²⁶, respectively. Ser⁷²⁶ resides within a putative CKII/protein kinase A phosphorylation site located upstream to a dileucine motif with yet undefined function (*underlined and bold*). In *pIgR-S726-t*, the codon encoding Ser⁷²⁶ has been mutated to a stop codon, resulting in the deletion of the C-terminal 30 amino acids in the cytoplasmic tail. *CD-MPR*, the basolateral sorting signal is close to the transmembrane domain and is similar to that of the *pIgR*. It contains a putative RXXV sequence (74). Phosphorylated Ser in a CKII phosphorylation site (*bold and underlined*) is proposed to mediate AP-1 binding (32). The downstream dileucine-based motif (*underlined*) may play a role in sorting from the TGN to endosomes or from endosomes to the cell surface. Amino acids are indicated with the single-letter codes.

MDCK cells grown on 12-mm Transwell filters were pulse-labeled for 10 min at 37 °C with [³⁵S]Cys, Met (0.07 mCi of Promix; Amersham Pharmacia Biotech) and subsequently chased for 15 min at 37 °C in minimal essential medium containing bovine serum albumin (MEM-BSA) (MEM containing Hanks' balanced salt solution (Sigma), 20 mM Hepes, pH 7.4, and 0.6% BSA) lacking radioactive amino acids. To label apical endosomes, WGA-HRP (12 μg/ml) or free HRP (10 mg/ml) was introduced into the medium bathing the apical surface during the chase at 37 °C. To label basolateral early endosomes, free HRP (10 mg/ml) was added to the medium in the basolateral chamber during the 15-min chase. In all cases, the medium in contact with the basolateral surface was supplemented with V8 proteinase (Roche Molecular Biochemicals) throughout the entire chase period. The proteinase does not digest HRP, but it immediately digests the luminal domain (*i.e.* the SC) of radiolabeled *pIgR* molecules that appear on the basolateral plasma membrane. V8-digested *pIgR* is no longer recognized by anti-SC antibodies and cannot be immunoprecipitated from the cell (our proteinase-based delivery assay is based upon this principle (29)). The application of V8 proteinase was important for preventing the internalization of intact molecules into the cell, thereby eliminating the ability of exocytic receptors to reach endosomes via the indirect post-endocytic route. In cases where a fraction of metabolically labeled *pIgR* reaches the apical surface, apical endocytosis of surface arriving receptor molecules is largely diminished because of efficient cleavage of *pIgR* to SC by the endogenous protease. Cells were then washed three times quickly and once for 5 min with ice-cold MEM-BSA containing 20% calf serum to quench the V8 proteolytic activity. Noninternalized HRP was stripped from the cell surface as follows: WGA-HRP was removed by incubating the cells with 100 mM *N*-acetyl-D-glucosamine in ice-cold MEM-BSA for three times for 10 min each time. HRP was removed by washing the cells twice quickly and once for 60 min with ice-cold glycine buffer (150 mM NaCl, 2 mM CaCl₂, 10 mM glycine, pH 9.0) as described (44). Cells were then washed twice with ice-cold MEM-BSA, medium was aspirated, and DAB reaction buffer (0.5 ml) was added to both the apical and basolateral compartments of the Transwell. The DAB reaction buffer was prepared by adding 1.65 ml of 3 mg/ml DAB to 10 ml HBSS⁺ (1.3 mM CaCl₂, 0.4 mM MgSO₄, 5 mM KCl, 5.6 mM D-glucose, 25 mM Hepes titrated to pH 7.4 with NaOH). The pH of the solution was then carefully adjusted to 7.0 with NaOH, filtered through a 0.45-μm pore filter unit, and 12 μl of fresh 30% H₂O₂ was added to the DAB reaction buffer. In control experiments, H₂O₂ was omitted from the DAB reaction buffer. Upon

incubation with monomeric DAB and peroxide, DAB is selectively polymerized by the peroxide. Consequently, peroxide-containing organelles become detergent-insoluble. Following 45 min of incubation at 4 °C, cells were washed twice with ice-cold HBSS⁺, buffer was aspirated, and filters were excised from their holders, boiled for exactly 90 s in 0.5 ml of SDS-lysis buffer (0.5% SDS, 100 mM NaCl, 50 mM triethanolamine chloride, pH 8.6, 5 mM EDTA, 0.02% (w/v) sodium azide) containing 1 mM phenylmethylsulfonyl fluoride. Filters in lysis buffer were then vortexed for 15 min at 22 °C, and SDS-insoluble DAB polymers were pelleted by centrifugation (100,000 × *g*, 4 °C, 25 min, TL-100 Beckman ultracentrifuge). Supernatants were added to 0.5 ml of 2.5% Triton dilution buffer (TDB) (100 mM NaCl, 5 mM EDTA, 100 mM triethanolamine chloride, pH 8.6, 2.5% Triton X-100, 0.02% sodium azide), and the *pIgR* was immunoprecipitated with sheep anti-rabbit SC polyclonal antibodies covalently coupled to protein A-Sepharose (50 μl of 15% slurry) as described (37). The immunoprecipitated protein was analyzed by SDS-PAGE and autoradiography. The *pIgR* was immunoprecipitated, and the degree of *pIgR* meeting with endosomes is calculated from the relative loss in radiolabeled receptor signal (see Fig. 3A).

Determination of Cell-associated HRP Activity—Internalization of large HRP concentrations may result in nonspecific precipitation of metabolically labeled *pIgR*. We hence carefully calibrated the concentration of HRP ligands applied to the cells in each experiment, and the concentration chosen (mentioned above) resulted in the consistent internalization of HRP activity that did not cause the pelleting of pulse-labeled receptors (namely, receptors located in the endoplasmic reticulum).

Cell-associated HRP activity in each experiment was determined using the following protocol. HRP-coupled ligands or free HRP was internalized from the apical surface of MDCK cells, and surface-bound ligand was removed. Cells were washed twice quickly with ice-cold phosphate-buffered saline, the filter was excised from its holder, and cells were scraped into 0.1 ml of ice-cold TDB containing 2.5% Triton X-100 lacking sodium azide. Cell lysates were vortexed at 4 °C for 20 min, and 1 ml of phosphate-buffered saline containing 0.75 mg/ml *o*-phenylenediamine dihydrochloride (Sigma) and 0.023% H₂O₂ was added to the lysate. The mixture was incubated further for 20 min on ice, and the reaction was stopped with 0.3 ml of 1 N HCl. Absorbance was determined at 492 nm, and the amount of cell-associated HRP was derived from a standard calibration curve using 1–50 ng of free HRP. Uptake of WGA-HRP at 37 °C or at 17 °C from the apical surface of

filter-grown MDCK cells resulted in the internalization of ~30 ng of HRP. Fluid phase uptake of free HRP at 37 °C caused reproducible internalization of 30–50 ng of HRP activity. Only about 1% of pulse-labeled receptors was pelleted after ligand binding to the apical surface at 4 °C (resulting in >50 ng of cell-associated HRP activity), confirming that radiolabeled receptors are not shifted by nonspecific association with DAB polymers after lysis of cells in SDS.

Meeting of Post-endocytic Receptors with Apically Endocytosed WGA-HRP or Free HRP—Cells expressing the pIgR cultured on 12-mm Transwells were placed on 30- μ l drops of MEM-BSA containing 10 μ g/ml 125 I-labeled Fab fragments (Fabs produced from guinea pig anti-SC antibodies were iodinated by the iodine monochloride method (8)) yielding specific activity of 2×10^7 cpm/ μ g protein, and ligand was allowed to internalize from the basolateral surface for 30 min at 37 °C. During the last 15 min of Fab internalization, WGA-HRP or fluid phase HRP were internalized from the apical surface. Surface-bound ligand was removed, and DAB reaction was initiated with H₂O₂ in one set of filters, whereas H₂O₂ was omitted in control filters. Cells were solubilized in 0.5 ml of SDS-lysis buffer, lysates were boiled for 90 s, and SDS-insoluble DAB polymers were pelleted by centrifugation (100,000 \times g, 25 min, 4 °C, TL-100 Beckman ultracentrifuge). Radioactivity level associated with SDS-soluble material in the supernatant (X) was determined by a γ -counter. MDCK cells that do not express the pIgR were analyzed in parallel to control for nonspecific uptake of ligand, and the values obtained were subtracted as background (never more than 7% of the signal from pIgR-expressing cells). Each experiment was performed in triplicate, and the level of meeting was deduced from the percent of reduced radioactivity in treated (+H₂O₂) compared with nontreated cells (-H₂O₂), using the equation presented in the legend to Fig. 3A (see also Fig. 8A). In cases where meeting with hTfn was examined, PTR cells were first depleted of endogenous Tfn by incubating the cells for 4 h at 37 °C in MEM-BSA. Human apo-transferrin (Biological Industries, Beit Haemek, Israel) was loaded with iron (38) and iodinated by the iodine monochloride technique to yield approximately 10 μ g/ml 125 I-labeled hTfn at 7×10^6 cpm/ μ g specific activity. Ligand was continuously internalized from the basolateral surface of PTR cells for 30 min at 37 °C to allow the labeling of ARE or CE (19), and its association with apically endocytosed HRP was determined as described above for pIgR labeled with 125 I-Fabs.

Trafficking Assays

Basolateral Delivery—The rate of newly synthesized pIgR delivery to the apical or basolateral cell surface of MDCK cells, in the absence or presence of BFA, was determined quantitatively by the protease-based delivery assay (29). A biotinylation-based assay for cell surface delivery was used to assess the targeting of newly synthesized hTfnR to the basolateral and apical cell surface. PTR cells cultured on 12-mm filter supports were pulse-labeled for 15 min at 37 °C, washed, and then chased for 7, 15, 30, or 60 min at 37 °C in MEM-BSA. At the end of each chase time, cells were washed three times with ice-cold HBSS⁺ adjusted to pH 7.4. Proteins at the apical and basolateral cell surface were biotinylated with NHS-LC-biotin (500 μ g/ml; Pierce) on ice for 15 min. Biotinylation was repeated, and cells were subsequently washed three times for 5 min each time with MEM-BSA supplemented with 50 mM glycine. Cells were then lysed in 2.5% TDB containing a mixture of protease inhibitors, and the hTfnR was immunoprecipitated using H68.4 monoclonal antibodies (45) coupled to protein A-Sepharose. After three washes with mixed micelle buffer (20 mM triethanolamine chloride, pH 8.6, 150 mM NaCl, 5 mM EDTA, pH 8.0, 8% w/v sucrose, 0.1% Na₃, 1% w/v Triton X-100, 0.2% SDS) and one wash with final wash buffer (mixed micelle buffer lacking Triton X-100 and SDS), the immunobead suspension in final wash buffer was divided into two fractions, each of which was centrifuged. The bead pellet was processed as follows. Beads in one-fifth of the original volume were dissolved in SDS sample buffer; this fraction was used to determine the total amount of immunoprecipitated radiolabeled receptors. The remaining bead suspension was pelleted, boiled for 5 min in 20 μ l of 10% SDS, and biotinylated pIgR was precipitated by streptavidin agarose (50% slurry in 2.5% TDB; Sigma) as described (8). hTfnR precipitated from both fractions was analyzed by 10% SDS-PAGE, and radioactivity was quantified by the FUJIX BAS 1000 bioimaging system as described. In some experiments 10 μ g/ml BFA (EpiCenter; diluted from a 10 mg/ml stock solution in Me₂SO stored at -20 °C) was included into the apical and basolateral medium throughout the chase.

Steady-state Distribution—To evaluate the steady-state distribution of the hTfnR on the apical and basolateral plasma membranes of PTR cells, each cell surface was selectively biotinylated in the cold. After

three washes with MEM-BSA-glycine buffer, cells were lysed in TDB, and the hTfnR was immunoprecipitated. Immunoprecipitates were analyzed by SDS-PAGE electrotransferred to a nitrocellulose membrane (37), and the nitrocellulose membrane was incubated with a blocking buffer (37) lacking dry milk. Biotinylated receptors were detected with HRP-labeled streptavidin (Pierce, 1:1000 in TBST (10 mM Tris, pH 8.0, 180 mM NaCl, 0.05% Tween 20), 30 min at 22 °C) using a Luminol Reagent (Santa Cruz Biotechnology). The 90-kDa hTfnR band intensity was quantified (37).

Basolateral Recycling and Transcytosis—Basolateral recycling of hTfnR in PTR cells was monitored basically as described for the recycling of the endogenous dog transferrin (19). PTR cells were first depleted of endogenous Tfn by incubating the cells for 4 h at 37 °C in MEM-BSA. Cells were incubated from the basolateral side with 125 I-hTfn (10 μ g/ml at 7×10^6 cpm/ μ g specific activity) for 120 min at 18 °C. Cells were washed and incubated at 37 °C for 3, 7, 15, 30, 60, and 120 min in the absence of the radiolabeled ligand. At the various time intervals, cells were chilled, and the apical and basolateral media were harvested. Surface-associated hTfn was stripped by incubating the cells for 60 min at 4 °C in acidic glycine buffer (750 mM glycine, pH 2.5, diluted 1:5 in phosphate-buffered saline containing 0.6% BSA), and filters were then cut out of their holders. Radioactivity was determined for filters, the stripped fraction, and the basolateral and apical media. Constitutive transcytosis of empty pIgR was assessed using guinea pig anti-SC 125 I-Fab fragments as described (8), except that V8 proteinase (15 μ g/ml; Roche Molecular Biochemicals) was included into the basolateral medium throughout the various incubation times. It should be noted that although most of the nascent pIgR- Δ R655-Y668 or pIgR-R657,V660-AA are targeted from the TGN to the apical surface, a small fraction of these molecules is still directed to the basolateral surface, and the transcytotic activity of this fraction was monitored.

Immunofluorescent Labeling and Scanning Laser Confocal Microscopy

HRP coupled to fluorescein isothiocyanate (FITC) (5/mg/ml) or WGA-HRP (12 μ g/ml) was internalized from the apical surface for 15 min at 37 °C. Surface-bound ligand was stripped, and cells were fixed for 10 min in methanol at -20 °C (37), blocked and immunostained as described (19, 37). Internalized WGA-HRP was labeled with goat anti-HRP antibodies coupled to FITC (Jackson Immunochemicals; used at 1:250 dilution). The TGN was labeled with rabbit anti-TGN38 antibodies (at 1:250 dilution; kindly provided by G. Banting, University of Bristol) and donkey anti-rabbit secondary antibodies conjugated to Texas Red (Jackson Immunochemicals). The R40.76 anti-ZO-1 rat monoclonal antibody (46) (used at 1:250 dilution) with anti-rat-conjugated tetramethylrhodamine isothiocyanate (Jackson Immunochemicals) secondary antibody was used to label the tight junction-associated protein ZO-1. Secondary antibodies were used at the recommended dilutions.

A Bio-Rad MRC-1024 confocal scanhead coupled to a Zeiss Axiovert 135M inverted microscope was used to acquire images of the stained cells, with a 63 \times oil objective (numerical aperture 1.4). The instrument was configured for detection of three labels (FITC, tetramethylrhodamine isothiocyanate, and Texas Red) as described in Ref. 37. Data presented in this paper did not demonstrate colocalization of FITC and Texas Red, when analyzed as described in Ref. 37. However, that analysis was designed to provide a strict test for colocalization. Once colocalization was not observed, the analysis was modified to provide a strict test for lack of colocalization, as described below. All images were filtered with a 3 \times 3 median filter to remove point noise. Then the uniform background (estimated from areas of the field where there were no cells) was subtracted from each image. The FITC staining covered a wide dynamic range, so that some of the spots were saturated. Saturated areas of the images were discarded, because such signals are necessarily outside of the linear range of the detection system. Cross-talk between the FITC and Texas Red channels was negligible, as shown with control experiments. When testing for colocalization, an upper limit on cross-talk was used. However, to test for lack of colocalization, a lower limit on cross-talk (that is, zero) was used. Finally, the contrast was stretched to allow the stained areas to be easily seen. Areas of overlap of Texas Red and FITC appear yellow. There was no attempt to quantitate the relative strengths of the FITC and Texas Red emission. Images were saved in a tag information file format, and the contrast levels of the images were adjusted in the Photoshop 5.0 program (Adobe Co., Mountain View, CA) on a Power PC G3 Macintosh (Apple). The contrast corrected images were imported into Freehand (Macromedia, San Francisco, CA) and printed from a high quality color printer (Tektronix Phaser 440).

Electron Microscopic Analysis of Apically Endocytosed HRP Ligands

Following internalization of WGA-HRP or fluid phase HRP from the apical surface, cells were fixed for 30 min at 22 °C with a mixture of 2% paraformaldehyde 1% glutaraldehyde dissolved 0.1 M phosphate buffer (0.1 M NaH₂PO₄ and 0.1 M Na₂HPO₄, pH 7.4). Cells were rinsed three times in phosphate-buffered saline and then treated for 10 min at 22 °C with freshly prepared DAB solution (0.025% DAB (Sigma), 0.006% H₂O₂ in TBS (0.05 M Tris HCl, pH 7.4, and 0.9% (w/v) NaCl). Post-fixation was performed in a mixture of osmic acid tetroxide (1% v/v) and potassium ferricyanide (1.5% w/v) in cacodylate buffer (0.05 M sodium cacodylate pH 7.0) for 1 h at 22 °C. After brief washes in cacodylate, sections were dehydrated in ascending concentrations of ethanol and infiltrated with epoxy resin (EM-BED-812, Electron Microscopy Sciences). Flat embedding and ultrathin sectioning was performed as described elsewhere (47). Sections were viewed in a Philips 300 electron microscope.

RESULTS

Membrane-bound WGA-HRP and Fluid Phase HRP Internalized at 37 °C or at 17 °C from the Apical Membrane Do Not Co-localize with the Golgi System—We assayed the extent to which newly synthesized proteins meet with free HRP or HRP-coupled ligands internalized into endosomes. A prerequisite for this assay is to exclude the possibility that apically internalized ligands access the Golgi complex or the TGN compartment. It is well established that after short periods of internalization, free HRP taken up by fluid phase endocytosis enters into the vesicular portion of early sorting endosomes, and in polarized MDCK cells this marker can be selectively internalized into distinct apical and basolateral early endosomes (48, 49). On the other hand, general membrane-bound tracers like ricin and WGA have been used to label tubulovesicular recycling endosomes of nonpolarized cells and ARE of epithelial cells (19, 20, 50–52). We used morphological and biochemical approaches to confirm that in our experimental system, apically internalized WGA-HRP or fluid phase HRP indeed reach endosomes but not the Golgi/TGN compartments.

WGA-HRP or free HRP were internalized from the apical surface for 15 min at 37 °C, and surface-bound ligand was removed. Cells were fixed and co-stained with specific anti-HRP and anti-TGN38 antibodies followed by FITC or Texas Red-coupled secondary antibodies, respectively. The localization of HRP labeling with respect to the TGN marker, TGN38, in the apical-basal axis of the cell was recorded by scanning laser confocal microscopy. Confocal images clearly show that HRP-FITC produced very intense punctate staining, most likely because of ligand entering into the vesicular portion of early apical endosomes. WGA-HRP-FITC, in contrast, produced more extended staining patterns, probably because it is concentrated into tubular extensions of sorting endosomes and/or because of its entering the tubular portion of ARE or CE residing underneath the apical plasma membrane (Fig. 2A). At the same time, the anti-TGN38 produced a more widely distributed reticular staining. In all cases, HRP-FITC labeling appeared in focal planes above the tight junctions, whereas the TGN38-TR was seen in the plane of the tight junction and below (basolateral). Furthermore, even near the tight junctions, where very low HRP-FITC labeling and intense TGN38-TR labeling appeared in the same focal plane, there was practically no overlap between them. These data suggest that internalized ligands label morphologically distinct endosomal compartments at the apical pole of the cells and that they do not reach the TGN. Similar results were obtained after apical internalization of HRP ligands for 90 min at 17 °C (not shown). Here it is important to note that internalized WGA likely labels various apical endosomal compartments, including the CE or the ARE, but fluid phase HRP labels primarily early endosomes.

Next we analyzed the localization of internalized ligands with respect to the Golgi apparatus using high resolution electron microscopy. WGA-HRP or free HRP were internalized from the apical surface as before, and cells were processed for electron microscopy (Fig. 2B). Both ligands labeled organelles residing in the apical cytoplasm, some of which are in proximity to the Golgi apparatus. However, in more than 20 sections in each case, HRP reaction product was never found to label Golgi cisternae, suggesting that internalized ligands reside predominantly in the lumen of endosomes.

Finally, we used the density shift meeting assay to assess the ability of internalized tracers to access the TGN. WGA-HRP was internalized from the apical surface for 15 min at 37 °C, surface-bound lectin was removed, and HRP-mediated DAB polymerization was either induced (+) or not (–) with H₂O₂. Cells were solubilized in SDS, insoluble-shifted material was removed by centrifugation, and TGN38 was immunoprecipitated from the soluble fraction. We found that comparable amounts of TGN38 were immunoprecipitated from the induced and noninduced cells (Fig. 2C), suggesting that internalized ligand does not reach significant portions of TGN38-containing organelles in steady state. Similar data were obtained with free HRP (not shown). From the biochemical and morphological observations we conclude that apically internalized WGA-HRP or free HRP reach apical endosomes but not the Golgi apparatus or the TGN.

The Biosynthetic Pathway to the Basolateral Surface Passes through Apical and Basolateral Endosomes—Our first aim was to analyze the direct delivery of newly synthesized pIgR-WT to endosomes. The exocytic transport of the pIgR from the TGN to the basolateral cell surface was followed by pulse labeling of pIgR-expressing MDCK cells with ³⁵S-labeled methionine and cysteine for 10 min and chased for 15 min in medium that lacked the radiolabeled amino acids. During the chase, V8 proteinase was added to the basolateral medium. The proteinase digested surface arriving pIgR molecules, thereby eliminating the ability of exocytosing molecules to reach endosomes via the post-endocytic pathway (see “Experimental Procedures”). We found that after pulse labeling and 15 min chase, only about 20% of radiolabeled pIgR-WT accessed the basolateral cell surface, and none could be detected in the apical plasma membrane (37). Thus, we thought that this chase period was appropriate for monitoring the fraction of newly made pIgR that is targeted directly to endosomes. Concomitant with the chase, WGA-HRP or free HRP was internalized from the apical surface, and the extent to which nascent pIgR meets with apically internalized ligand was assayed by the DAB-H₂O₂-induced density shift of organelles containing HRP as described under “Experimental Procedures” and in Fig. 3A. The average of several such experiments is shown in Fig. 3B.

After 10 min of pulse and 15 min of chase, ~30% of pulse-labeled pIgR reaches apical endosomes containing WGA-HRP, and less than 10% accesses free HRP taken up by fluid phase endocytosis (Fig. 3B, *Pulse+Chase*). Because ARE and CE can be accessed by membrane-bound endocytic ligands but are largely devoid of fluid phase endocytic tracers, these results suggest that newly synthesized pIgR is targeted from the TGN to a population of apical endosomes that probably correspond to ARE and CE, prior to reaching the basolateral plasma membrane. Interestingly, however, ~30% of newly synthesized pIgR also seems to meet with fluid phase HRP internalized from the basolateral surface. Fluid phase markers are thought to label primarily early sorting endosomes (e.g. the early endosomal rab5a has been co-localized with internal fluid phase markers (53)); thus, the exocytic pathway taken by pIgR-WT inefficiently traverses AEE but may include BEE.

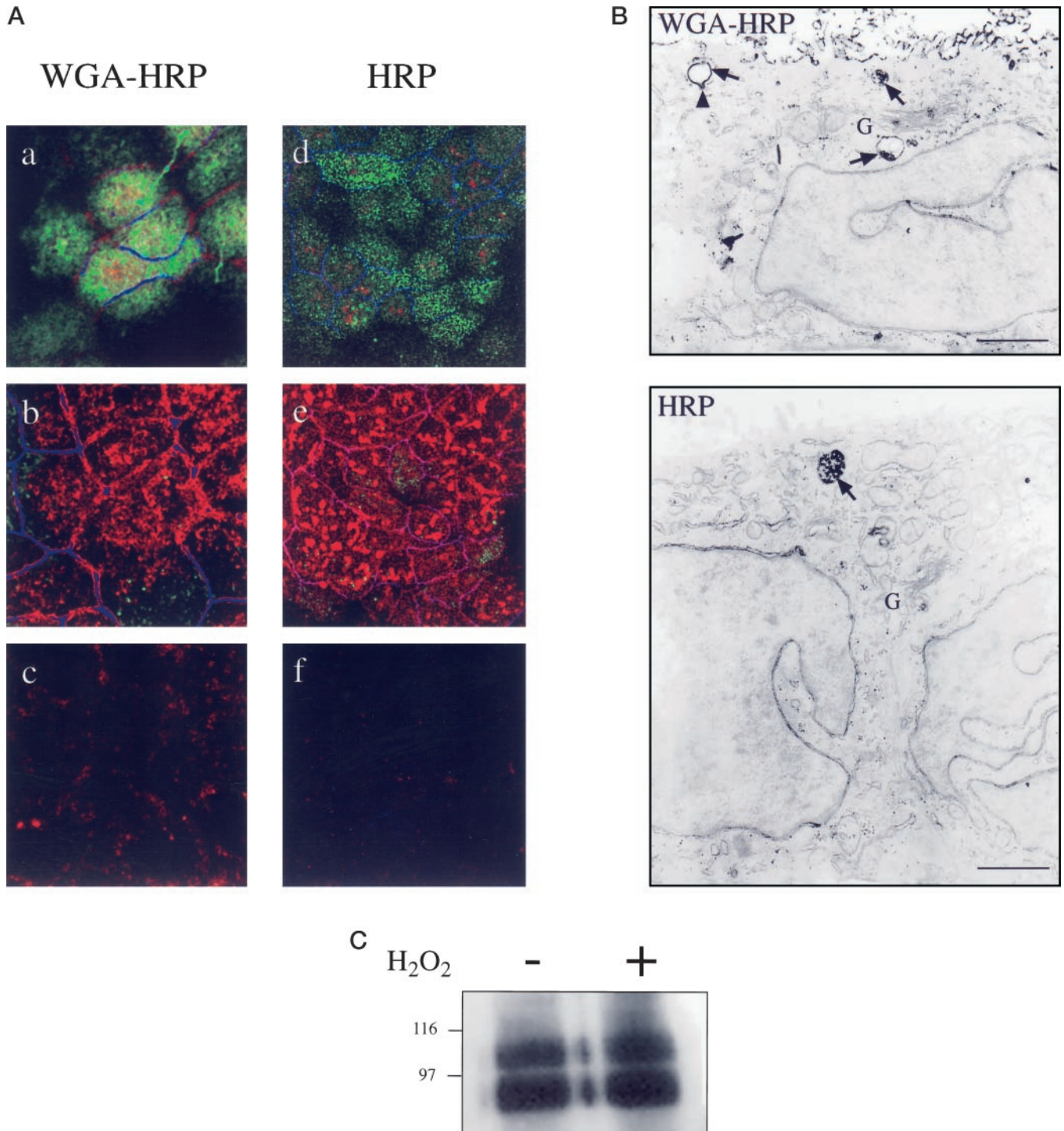


FIG. 2. Morphological and biochemical analyses of intracellular localization of apically internalized WGA-HRP and fluid phase HRP with respect to the Golgi apparatus. *A*, analysis by scanning confocal microscopy. WGA-HRP (*a-c*) or fluid phase HRP covalently coupled to FITC (*d-f*) was internalized from the apical surface of filter-grown MDCK cells for 15 min at 37 °C, and membrane-bound ligand was removed. Cells were fixed and co-stained with anti-HRP (in the case of WGA-HRP), anti-TGN38, and anti-ZO-1 primary antibodies followed by FITC (green), Texas Red (red), and tetramethylrhodamine isothiocyanate-conjugated (blue or red) secondary antibodies, respectively. The apico-basal axis of the cells was scanned by confocal microscopy. Representative optical sections taken from the apical pole above the ZO-1 belt (*a* and *d*), below ZO-1 but above the nucleus (*b* and *e*) and at the nucleus level (*c* and *f*), are shown. *B*, survey transmission electron micrograph of a filter-grown MDCK cells after incubation with WGA-HRP and HRP for 15 min at 37 °C at the apical surface. After ligand internalization, only surface-bound HRP was stripped from the apical plasma membrane. Cells were fixed and processed for electron microscopy. A continuous coat of DAB polymer formed in the exoplasmic face of HRP-labeled endosomes (marked with arrows) is detected mostly at the apical cytoplasm, above the nucleus. Occasionally these endosomes are seen in the vicinity to Golgi stacks (*G*), but those stacks were not apparently labeled with DAB. Endosomal elements resembling vacuoles of ~0.3 μ m with a tubular extension were also seen (arrowhead). Note that apical endosomes with a similar shape have been reported to contain both basolateral and apical recycling Tfn and IgA, respectively (15). Bar, 1 μ m. *C*, apically internalized WGA-HRP does not reach TGN38-containing membranes. WGA-HRP was internalized from the apical surface, and surface-bound ligand was removed. Cells were treated with DAB, and DAB polymerization was induced (+) or not (-) by H₂O₂. Cells were solubilized in SDS, DAB polymers were removed by centrifugation, and TGN38 was immunoprecipitated from the supernatant using 2 μ l of rabbit antiserum. Immunoprecipitates were analyzed by SDS-PAGE and Western blotting with enhanced chemiluminescence. The signal level of immunoprecipitated protein band corresponding to the TGN38 (a ~100-kDa doublet (75)) was quantified by NIH image. Molecular mass markers are indicated in kDa.

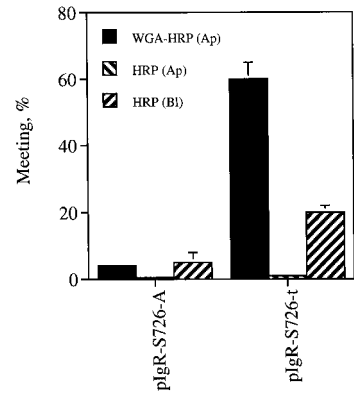
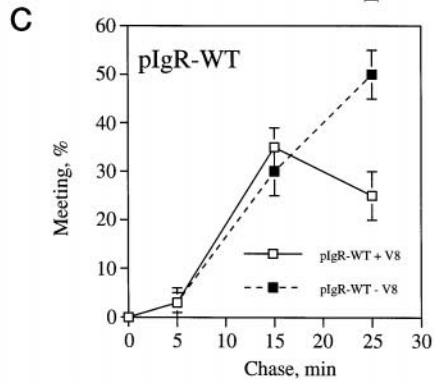
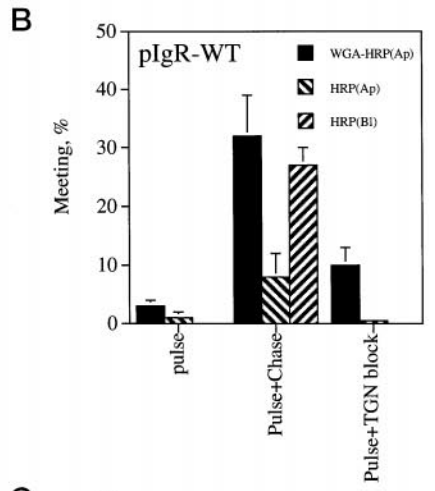
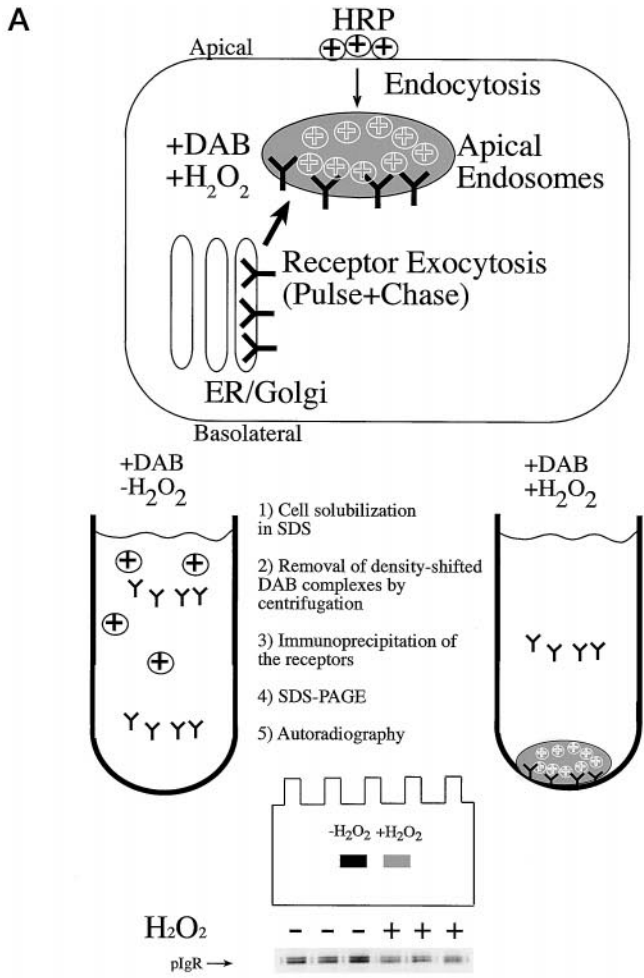


FIG. 4. Targeting of newly synthesized pIgR-S726-A and pIgR-S726-t to apical endosomes. The meeting of pulse-labeled pIgR mutants with apically endocytosed WGA-HRP or with apically or basolaterally endocytosed free HRP was examined after 15 min chase at 37 °C. Results are the means ± S.E. of three experiments.

Pulse-labeled pIgR is located in the endoplasmic reticulum and is sensitive to digestion by endoglycosydase H (23). In contrast, after pulse and 90 min of chase at 17 °C, the pIgR is blocked from exiting the TGN, and it acquires resistance to digestion by the enzyme (23). In both cases, the pIgR should not meet ligands in endosomes. Cells were pulse-labeled for 10 min or pulse-labeled and then chased for 90 min at 17 °C. WGA-

FIG. 3. Targeting of newly synthesized pIgR-WT to apical and basolateral endosomes. A, schematic presentation of the assay used to measure the targeting of biosynthetically labeled pIgR to apical endosomes. Receptors in filter-grown MDCK cells were pulse-labeled and briefly chased under conditions that did not allow them to reach endosomes after internalization (see “Experimental Procedures”). During the chase, endocytic ligands bearing HRP (depicted as ⊕) were internalized from the apical surface to label apical endosomes or from the basolateral plasma membrane to label basolateral endosomes (not shown). The density of endosomes was shifted by HRP-catalyzed DAB polymerization (labeled with gray) induced with peroxide (+H₂O₂). Consequently, HRP-containing organelles become detergent-insoluble. The protein content of density-shifted organelles, which in our experiment may contain metabolically labeled receptors, cannot be extracted and simply analyzed by immunoprecipitation. However, the fraction of receptor reaching HRP-containing endosomes is determined indirectly. Density-shifted or nonshifted control cells were solubilized in SDS, and density-shifted material (endosomes) was removed by centrifugation. Radiolabeled receptors were immunoprecipitated from the supernatants, and immunoprecipitates were resolved by SDS-PAGE followed by autoradiography. Receptor band intensity was quantified by densitometric scanning. If metabolically labeled receptors reach HRP-containing endosomes, a loss in radiolabeled receptors is observed following cell solubilization and receptor immunoprecipitation from density-shifted cells (+H₂O₂), by comparison to control cells that were not shifted (-H₂O₂) (compare pIgR band signal in +H₂O₂ versus -H₂O₂ in the representative autoradiogram). The reduction is due to receptor entrapment in DAB polymers and removal upon centrifugation. Therefore, the fraction of radiolabeled receptors delivered to endosomes is inversely proportional to the reduced signal contributed by pIgR immunoprecipitated from the density-shifted cells. The level of [³⁵S]pIgR meeting with endosomes is calculated using the following equation: Meeting, % = 100 × [1 - (X⁺H₂O₂/X⁻H₂O₂)], where X is the band signal of pIgR in density-shifted (+H₂O₂) and nonshifted (-H₂O₂) cells. B, quantitative analysis of the targeting of newly made pIgR-WT to apical (Ap) endosomes loaded with WGA-HRP or with free HRP or to basolateral (Bl) endosomes harboring fluid phase HRP. pIgR-WT expressed in filter-grown MDCK cells was either pulse-labeled for 10 min at 37 °C (Pulse), pulse-labeled and chased for 15 min at 37 °C (Pulse+Chase), or pulse-labeled and chased for 90 min at 17 °C (Pulse+TGN block). Ligands were internalized either from the apical or from the basolateral plasma membrane during the pulse, pulse and chase, or pulse and TGN block periods, and the percentage of meeting was determined. Results are the means ± S.E. of at least six independent experiments, each of which performed in triplicate. C, time course of pIgR-WT meeting with apically internalized WGA-HRP. Meeting was examined after pulse and 5, 15, and 25 min of chase. In all cases, WGA-HRP was internalized for 15 min at 37 °C. Results are the means ± S.E. of three experiments.

HRP was internalized during pulse-labeling or during the 90-min chase, and the fraction of metabolically labeled pIgR pelleted with HRP-containing apical endosomes was measured. Results presented in Fig. 3B reveal that less than 5% of pulse-labeled pIgR meets with HRP tracers internalized during pulse labeling. Approximately 10% of the pulse-labeled pIgR appeared to associate with HRP-containing endosomes after 90 min chase at 17 °C. Collectively, these results are consistent with the expectation that newly synthesized pIgR in the endoplasmic reticulum or Golgi does not meet HRP-coupled ligands in endosomes and further confirm the reliability of the assay in detecting receptor meeting with endosomes. However, ~30% meeting was obtained if pulse-labeled pIgR was incubated for 90 min at 17 °C and subsequently chased for 15 min at 37 °C with WGA-HRP internalized from the apical surface during the 15 min chase (not shown). In this case, meeting is likely contributed by direct delivery of the pIgR from the TGN to apical endosomes. In summary, the results so far indicate that in the course of exocytosis, pIgR-WT is targeted from the TGN to at least two types of endosomal populations: apical endosomes (presumably ARE and/or CE) and BEE.

Kinetics of pIgR Delivery to Endosomes—The degree of meeting between metabolically labeled pIgR and endosomes should vary as a function of chase time. Short periods of chase should result in low meeting levels because the cohort of metabolically labeled receptors has not yet entered endosomes. Meeting levels should reach maximal levels and then decrease at longer chase periods as a result of [³⁵S]pIgR entering and subsequently leaving endosomes *en route* to the cell surface. These predictions have been tested by measuring the meeting levels between pulse-labeled pIgR and apically endocytosed WGA-HRP after 5, 15, and 25 min of chase in the presence of basolateral V8 proteinase. In each chase period, WGA-HRP was consistently internalized from the apical surface for 15 min. Data in Fig. 3C agree with the above expectation; after 5 min chase only 3% of [³⁵S]pIgR was associated with endosomes. The meeting levels peaked to approximately 35% after 15 min chase and subsequently decreased to ~25% following 25 min of chase.

Previously, it was shown that after a 25-min chase, approximately 40% of pulse-labeled receptors reaches the basolateral surface (37). In the absence of basolateral V8, a fraction of these receptors would internalize and reach apical endosomes via the indirect transcytotic route. In this case, meeting levels are expected to increase because apical endosomes can now be reached by [³⁵S]pIgR traveling in the direct (biosynthetic) and indirect (transcytotic) routes. Data in Fig. 3C indeed show that in the absence of V8, meeting levels are doubled (from 25 to 50%) after 25 min of chase, suggesting that apical endosomes can also be accessed by receptors traveling in the post-endocytic, *e.g.* transcytotic, route. This possibility is further investigated below.

The Biosynthetic Route of pIgR-S726-A Circumvents Endosomes, Whereas Exocytosing pIgR-S726-t Is More Efficiently Targeted to Apical Endosomes—It has been previously suggested that pIgR-S726-A and pIgR-WT utilize BFA-insensitive and BFA-sensitive routes from the TGN to the basolateral surface, respectively (37). We examined the possibility that these mechanistically distinct exocytic routes may also be distinguished by their ability to access endosomes. In Fig. 4 we show that after pulse and 15 min of chase, ~1% of pIgR-S726-A meets with apically internalized WGA-HRP, and about 5% of radiolabeled receptors are associated with apically or basolaterally internalized fluid phase HRP. Thus, after the indicated chase period, insignificant levels of newly synthesized pIgR-S726-A appeared to reach endosomes. However, it should be noted that after 15 min of chase the pIgR-S726-A mutant

barely reaches the basolateral surface (37). Hence, it is plausible that longer chase times are required to transport [³⁵S]pIgR-S726-A to endosomes. However, this does not seem to be the case because no meeting with either tracer could be observed even after 25 min of chase (not shown), when ~30% of the pulse-labeled pIgR-S726-A appeared to reach the basolateral cell surface (37). These results strongly imply that pIgR-S726-A utilizes an alternative basolateral exocytic route that does not involve endosomes.

The data presented so far suggest that membrane proteins that take a slower and BFA-insensitive route bypass endosomes, whereas proteins taking a faster and BFA-sensitive pathway to the cell surface utilize endosomes. If this correlation were true, we expect that a pIgR mutant whose targeting to the basolateral cell surface occurs with faster kinetics will be more sensitive to BFA and meet endosomes more efficiently than pIgR-WT. An earlier work has shown that basolateral exocytosis of the truncated pIgR mutant, pIgR-S726-t (see also Fig. 1), occurs at significantly higher rate than pIgR-WT (42). For example, after 15 min of chase, 20% of [³⁵S]pIgR-WT was detected on the basolateral plasma membrane compared with ~50% of [³⁵S]pIgR-S726-t. Interestingly we find that basolateral delivery of pIgR-S726-t was also more potently inhibited by BFA; after 60 min chase ~40% of [³⁵S]pIgR-WT reached the basolateral plasma membrane of BFA-treated MDCK cells (30), whereas 20% delivery of pIgR-S726-t is observed after the same chase time. Consistent with our expectation, results in Fig. 4 show that after 15 min of chase at 37 °C, ~60% of pulse-labeled pIgR-S726-t is targeted to WGA-HRP-loaded apical endosomes. These meeting levels are almost two times greater than those measured for pIgR-WT (Fig. 3B). The pIgR-S726-t mutant did not meet with apically internalized HRP. Together, these results suggest a correlation between the efficiency of exocytosis and meeting with apical endosomes.

The Biosynthetic Route of hTfnR Traverses Apical Endosomes—We next investigated whether the convergence of the biosynthetic and endocytic pathways represents a general phenomenon and encompasses other basolateral receptors, such as the hTfnR. To investigate this possibility, we isolated an MDCK cell line in which we co-expressed the pIgR and the hTfnR (called PTR). In this cell line, approximately 80% of surface-associated hTfnR is localized on the basolateral plasma membrane and 20% in the apical domain (Fig. 5A), and the hTfnR is predominantly delivered from the TGN to the basolateral surface (Fig. 5B). In addition, basolateral transport of newly synthesized hTfnR is significantly inhibited by BFA (Fig. 5B).

PTR cells were pulse-labeled, and the meeting of radiolabeled pIgR and hTfnR with WGA-HRP or fluid phase HRP internalized from the apical plasma membrane was examined after 15 min of chase at 37 °C, with V8 protease included into the basolateral medium during the chase. Under these conditions, 40% of the radiolabeled pIgR and hTfnR were found to associate with apical endosomes bearing WGA-HRP, and a much smaller fraction (5–10%) accessed apical endosomes loaded with fluid phase HRP (Fig. 5C). These results suggest that the biosynthetic pathways of both the pIgR and hTfnR converge in apical endosomes and are consistent with previous observations showing that the biosynthetic pathway of hTfnR operates via endosomes in nonpolarized cells (10).

Apical Exocytosis of pIgR Mutants Occurs via Apical Endosomes—We next analyzed the possibility that apically sorted newly made pIgR mutants pass through endosomes. Two pIgR mutants, pIgR-ΔR655-Y668 and pIgR-R657,V660-AA (28, 30), were chosen for this purpose. Examination of the kinetics of their surface delivery revealed that after pulse and 15 min of

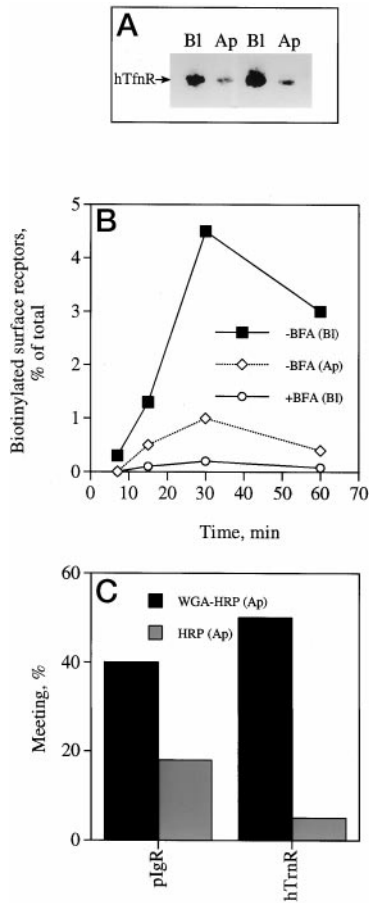


FIG. 5. Exocytic hTfnR is delivered to apical endosomes in polarized MDCK cells. *A*, steady-state distribution of hTfnR in two clones of polarized PTR cells. The steady-state cell surface expression of hTfnR in PTR9 and PTR10 cells cultured on filter supports was measured by domain-specific biotinylation-based assay. In both cases, about 80% of surface-expressed receptors are located on the basolateral (Bl) plasma membrane, and 20% is on the apical (Ap) plasma membrane. A representative result of an experiment performed in duplicate is presented. *B*, time course and BFA sensitivity of the delivery of newly synthesized hTfnR to the basolateral (Bl) or the apical (Ap) surface of PTR cells was examined by pulse-chase combined with surface domain-specific biotinylation as described under "Experimental Procedures." Cells were either treated (+) or not (-) with BFA. Results are the means of three measurements. *C*, meeting of biosynthetically labeled hTfnR and pIgR with apical endosomes. Cells were pulse-labeled and chased for 15 min at 37 °C with V8 proteinase in the basolateral medium. Targeting to apical endosomes labeled with WGA-HRP or fluid phase HRP was determined. Results are the means of two determinations.

chase, pIgR-R657,V660-AA does not appear on the apical cell surface, and only ~10% pIgR-ΔR655-Y668 accessed that surface (not shown). Neither receptor mutant could be detected on the basolateral plasma membrane after the indicated chase time.

pIgR-ΔR655-Y668 or pIgR-R657,V660-AA were pulse-labeled and chased for 15 min at 37 °C. WGA-HRP or fluid phase HRP was internalized from the apical surface during the chase, and the meeting of biosynthetically labeled receptors with ligand-containing endosomes was assessed by the DAB density shift assay. Results show that about 60% of pulse-labeled pIgR-ΔR655-Y668 or pIgR-R657,V660-AA meets with apical endosomes loaded with WGA-HRP (Fig. 6). The extent of meeting is almost 2-fold greater than that measured for pIgR-WT or hTfnR (Figs. 3*B* and 5*C*).

WGA-HRP is likely internalized into various apical endosomal compartments, including AEE. Thus, we suggest that higher meeting efficiency could be attributed to targeting of

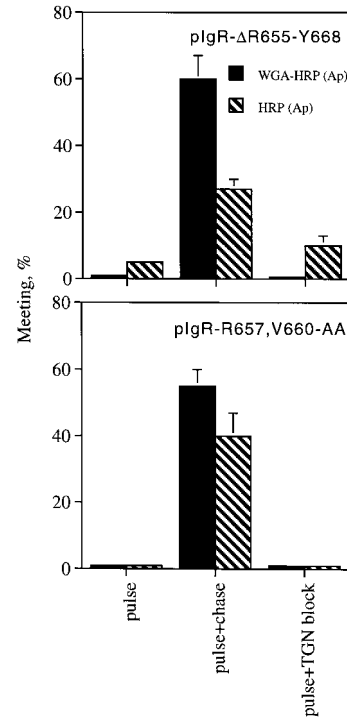


FIG. 6. The meeting of biosynthetically labeled apically sorted pIgR mutants with WGA-HRP or fluid phase HRP internalized from the apical surface. Targeting of newly synthesized pIgR-ΔR655-Y668 and pIgR-R657,V660-AA to apical endosomes bearing WGA-HRP or fluid phase HRP was examined. Results are the means ± S.E. of three measurements.

newly made pIgR mutants to apical endosomal populations that can be accessed by membrane-bound ligands (*e.g.* ARE and CE) and by fluid phase ligands, namely, apical early endosomes. One can distinguish early endosomes from CE or ARE, because only early endosomes can be accessed efficiently by fluid phase markers. If so, the exocytic road of apically sorted pIgR mutants should encounter HRP selectively internalized into AEE. To test this hypothesis, the targeting of newly made pIgR mutants with AEE loaded for 15 min at 37 °C with fluid phase HRP was examined. Data summarized in Fig. 6 indeed show reduced meeting levels (30–40%) of biosynthetically labeled pIgR mutants with fluid phase HRP in AEE.

Fluid phase tracers can be chased from early endosomes into late endosomes by incubating the cells for another 15 min at 37 °C in the absence of tracers (48). To elucidate whether apically sorted pIgR encounters early *versus* late endosomal compartments, HRP was continuously internalized during the 15-min pulse-labeling period, and 15 min of chase at 37 °C was performed in the absence of HRP. Under these conditions, <5% of metabolically labeled receptors intersect with the fluid phase tracer (not shown), suggesting that exocytic pIgR mutants meet with HRP in early endosomes. Taken together, the results suggest that the biosynthetic route of apically sorted receptors pass through at least two apical endosomal populations: endosomes accessed by membrane-bound ligands and endosomes accessed by fluid phase tracers (*i.e.* AEE).

Transcytosing Receptors Interact More Efficiently with Fluid Phase-containing Endosomes Than Do Basolateral Recycling Receptors—We measured recycling and transcytosis of the pIgR and hTfnR using anti-SC¹²⁵I-Fab fragments and ¹²⁵I-hTfn, respectively. The pIgR mutant pIgR-S664-A and hTfnR display efficient basolateral recycling and minor transcytotic activity (Fig. 7 and Ref. 27). Conversely, internalized pIgR-ΔR655-Y668 and pIgR-R657,V660-AA receptors efficiently transcytose from

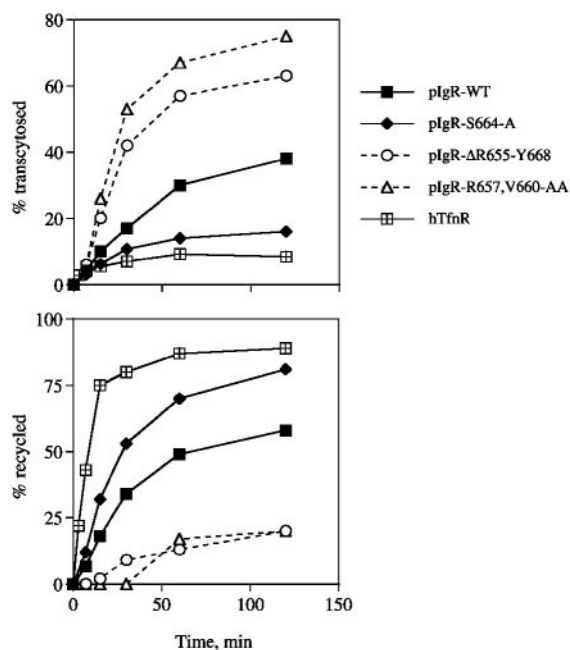


FIG. 7. Constitutive post-endocytic trafficking of pIgR and hTfnR. The constitutive basolateral recycling (% recycled) and basolateral-to-apical transcytosis (% transcytosed) over the indicated time periods of pIgR-WT, pIgR mutants, and the hTfnR expressed in PTR cells were measured as described under "Experimental Procedures." Results are the means of three experiments, each of which performed in duplicates. In most cases error bars are smaller than the symbol size.

the basolateral to the apical surface and poorly recycle to the basolateral plasma membrane (Fig. 7). Post-endocytic pIgR-WT exhibits an intermediate transcytotic/recycling phenotype (Fig. 7). If pIgR trafficking in the exocytic and post-endocytic pathways is regulated by a common mechanism (8), we expect that like basolaterally routed exocytic receptors, basolateral recycling receptors will encounter more efficiently apical endosomes loaded with WGA-HRP but not with fluid phase HRP. In contrast, analogous to apically targeted exocytic pIgR mutants, transcytosing receptors may meet endosomes loaded with both types of endocytic tracers. To test this hypothesis we measured the meeting of basolateral recycling and transcytosing receptors with apically internalized WGA-HRP or free HRP, using the DAB density shift protocol (see "Experimental Procedures" and Fig. 8A).

Data presented in Fig. 8B clearly reveal that ^{125}I -Fab continuously internalized from the basolateral surface by pIgR-S664-A-expressing cells or ^{125}I -hTfn internalized by PTR cells meet with apically internalized WGA-HRP but essentially not with fluid phase HRP. Conversely, ^{125}I -Fab internalized from the basolateral surface by cells expressing apically targeted pIgR mutants meet more efficiently with fluid phase HRP. Low meeting levels are also observed between transcytosing pIgR-WT and free HRP, whereas almost 60% of ^{125}I -Fab-labeled receptors meet with apically internalized WGA-HRP (Fig. 8B). These results suggest that the constitutive exocytic and transcytotic pathways taken by apically sorted pIgR involve AEE, whereas the basolateral pathway utilizes primarily ARE or CE but largely avoids AEE.

DISCUSSION

Our findings essentially argue that in polarized MDCK cells: (a) The BFA-sensitive exocytic road taken by basolaterally sorted pIgR involves apical endosomes that are not early endosomes (perhaps CE or ARE) and BEE. (b) Phosphorylated Ser⁷²⁶ in the cytoplasmic domain of pIgR is essential for receptor targeting from the TGN to endosomes; mutational inacti-

vation of this Ser confers pIgR incorporation into a BFA-insensitive basolateral route that also bypasses endosomes. Thus, membrane proteins can probably utilize mechanistically distinct but parallel exocytic routes and display variable ability in the extent to which they utilize endosomes during exocytosis. (c) The biosynthetic pathway of apically sorted receptors involves several apical endosomal populations, including AEE. (d) Transcytotic receptors taking the constitutive post-endocytic route traverse AEE, whereas basolateral recycling receptors interact with apical endosomes distinct from AEE. Thus, the exocytic and post-endocytic pathways of membrane proteins display a parallel phenotype with respect to their ability to interact with apical endosomes. The proposed pathways taken by the pIgR are summarized in Fig. 9.

We have recently suggested that the Golgi AP-1 adaptor complex interacts with the cytoplasmic domain of the pIgR and that these interactions are abolished when phosphorylated serine 726 is mutated to alanine (37). Because BFA causes AP-1 dissociation from Golgi membranes in MDCK cells, it is reasonable to assume that pIgR interactions with AP-1 on the TGN contribute to the BFA-sensitive basolateral transport of the receptor (30, 37, 54). These interactions may also play a role in pIgR targeting from the TGN to endosomes (Fig. 9, step 1). In contrast, the pIgR-S726-A mutant does not require AP-1 adaptors for its budding from the TGN. This mutant receptor hence buds into vesicles with distinct properties in a process that is BFA-insensitive and does not involve endosomes as an intermediate compartment (Fig. 9, step 9). Thus, phosphorylation of Ser⁷²⁶ is proposed to function as an important physiological switch for interactions of biosynthetic pIgR with specialized AP-1-coated areas in the TGN. These AP-1 adaptors are not involved in polarized sorting of the pIgR and thereby contain the $\mu 1a$ rather than the $\mu 1b$ subunit recently suggested to comprise an epithelial-specific AP-1 adaptor complex involved in basolateral sorting (55).

The phenomena described herein may not be restricted to the exogenously expressed pIgR in MDCK cells. The pathways taken by the pIgR-S726-A may correspond to basolateral trafficking pathways utilized by endogenous proteins, such as the BFA-insensitive basolateral pathway of uvomorulin in MDCK cells (56). We do not know whether the rate and BFA insensitivity basolateral transport of these proteins is modulated by CKII phosphorylation motifs. In fact, nor do we know the extent to which Ser⁷²⁶ to Ala mutation really mimics the state of nonphosphorylated serine. It is entirely possible that the mutation artifactually uncovers a nonphysiological sorting mechanism favoring the BFA-insensitive pathway. Nevertheless, it is worth noting that CKII phosphorylation of serines has been implicated in modulating the traffic of several proteins (32, 57–59). Thus, it is quite plausible that these motifs may also play a role in basolateral trafficking of endogenous as well as exogenously expressed membrane proteins.

Our data are consistent with previous observations indicating the existence of multiple distinct pathways (mechanisms) from the TGN to the apical (60, 61) and basolateral (62) plasma membrane. Another interesting case of parallel pathways has been documented for the targeting of soluble hydrolases to the vacuole in yeast. One of these pathways is regulated by the recently characterized AP-3 adaptor coat (63). Multiple redundant routes may hence function in higher as well as lower eukaryotes. In both cases the physiological significance of multiple routes is not clear. Parallel pathways may permit flexible regulation with respect to the efficiency of cargo sorting and targeting from the TGN to the basolateral plasma membrane, allowing cells to adjust sorting and targeting in response to changing physiological and developmental requirements. In

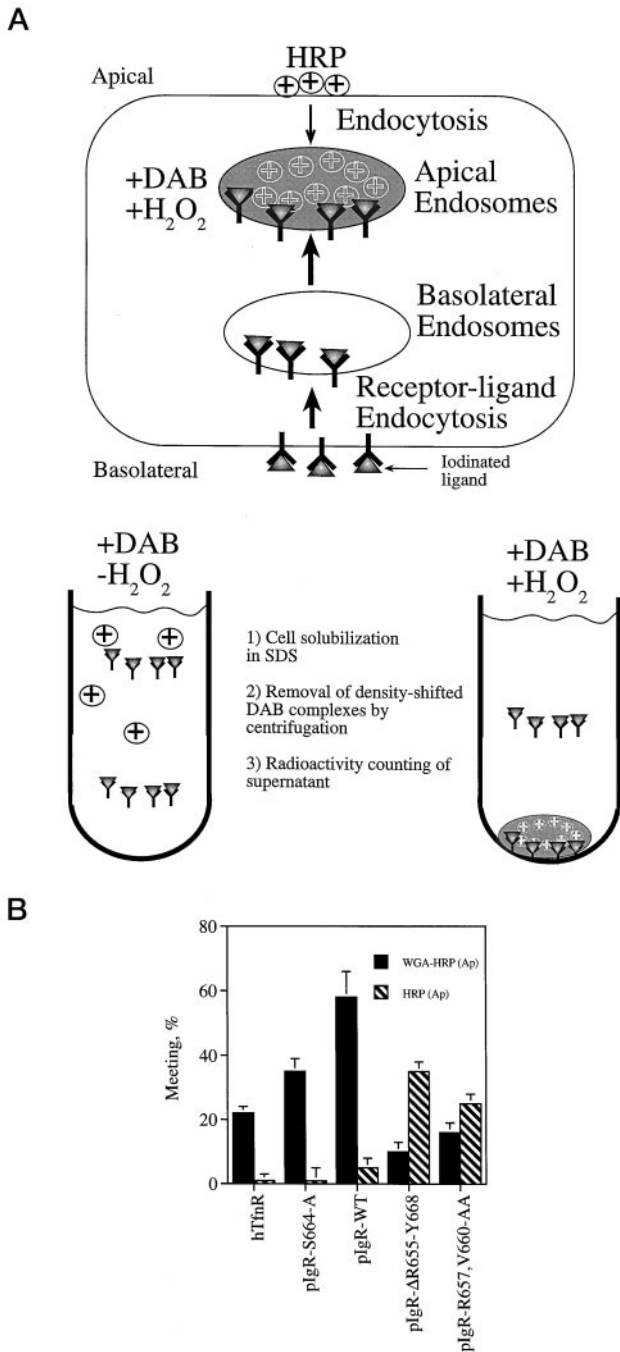


FIG. 8. The meeting of post-endocytic receptors with membrane-bound WGA-HRP and fluid phase HRP internalized into apical endosomes. *A*, schematic drawing of the assay. Basically, radiiodinated ligands (^{125}I -Fab fragments derived from anti-SC IgG or ^{125}I -hTfn) were internalized from the basolateral surface for 30 min at 37°C , and HRP (\oplus) was internalized for the last 15 min of this incubation into apical endosomes. Cells were then treated with DAB and peroxide ($+\text{H}_2\text{O}_2$) to induce DAB polymerization. In control cells peroxide was omitted and DAB polymerization was not induced ($-\text{H}_2\text{O}_2$). Following ligand stripping from the cell surface, cells were solubilized in SDS, and organelles containing DAB polymers were removed by centrifugation. Radioactivity in DAB-shifted and control samples was quantified by a γ -counter. *B*, quantitative analysis of meeting between basolateral recycling (hTfnR, pIgR-S664-A) or transcytotic receptors (pIgR-WT, pIgR- Δ R655-Y668, pIgR-R657,V660-AA) and apical endosomes loaded with WGA-HRP or fluid phase HRP. The percentage of ligand reaching endosomes was calculated from the reduction in radioactivity levels in peroxide-treated samples compared with control cells using the following equation: Meeting, % = $100 \times [1 - (\text{X}^+ \text{H}_2\text{O}_2 / \text{X}^- \text{H}_2\text{O}_2)]$, where X is the radioactivity signal in density-shifted and nonshifted cells. Results are the means \pm S.E. of two experiments performed in triplicates.

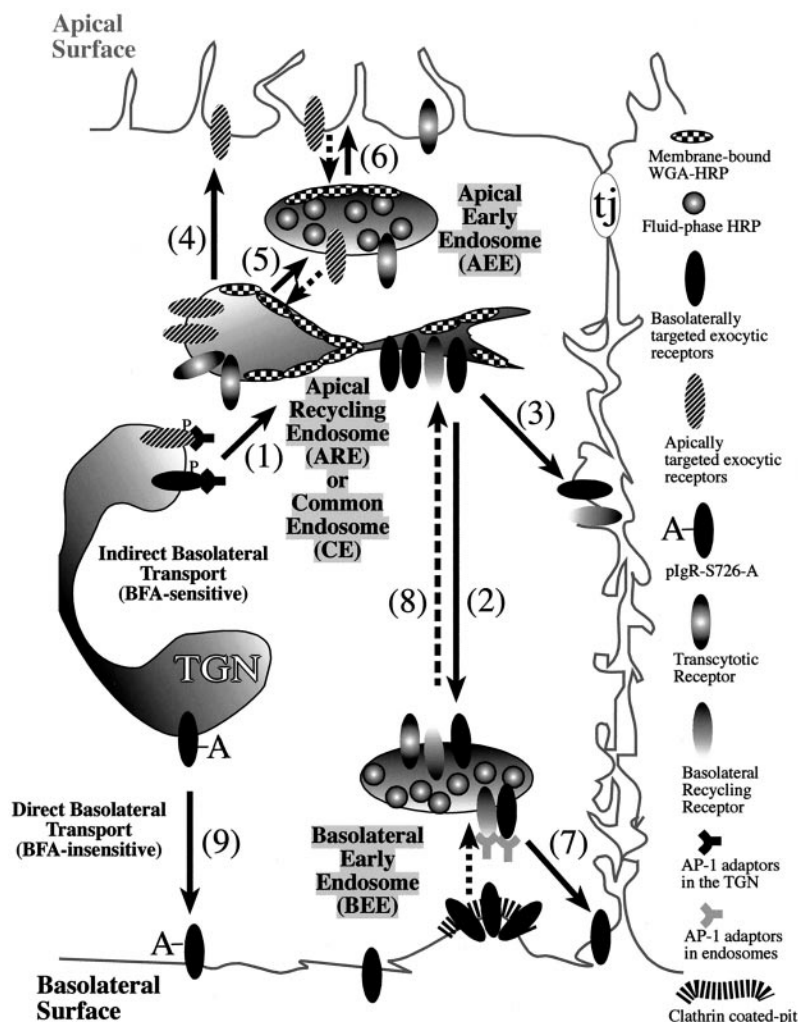
addition, redundant pathways may provide alternative modes of transportation in cases where one of the pathways is paralyzed.

Newly synthesized pIgR mutated in the basolateral sorting signal is routed to the apical surface via apical endosomes that include AEE prior to its appearance on the apical cell membrane (Figs. 6 and 9 *steps 1* and *5*). The Ser⁷²⁶ motif was kept intact in these mutants, and AP-1 adaptors may interact to some extent with this motif (37). The observation that apically and basolaterally sorted receptors meet with apically internalized membrane-bound ligand raises the intriguing possibility that the exocytic roads of these receptors merge into a common endosomal compartment, which could be the ARE or CE (Fig. 9, *step 1*). Consequently, certain steps in polarized sorting of these receptors may take place in endosomes. For instance, apical and basolateral proteins may be segregated from each other into discrete specialized populations of endosomes or alternatively into subdomains of individual endosomes specialized for basolateral or apical sorting (recycling). The existence of laterally segregated lipid microdomains in the membrane of tubulovesicular sorting endosomes (64) may contribute to membrane protein concentration into specialized distinct regions within this complex organelle. It is worth noting that although our data suggest that sorting in the biosynthetic pathway occurs in endosomes, we emphasize that they do not provide any direct evidence concerning the role of endosomes in polarized exocytosis. It seems equally likely, for instance, that exocytic wild-type receptors access endosomes and recycle back to the TGN, where the crucial sorting event may still take place. In this case, the observed propensity of different pIgR mutants to encounter the apical endosome could be explained by differences in the kinetics of recycling exhibited by the different mutants. Thus, additional experiments are needed to establish the precise intracellular site for polarized sorting.

Clathrin-coated buds containing γ -adaptin have previously been localized mainly on the TGN (65) but have also been found to be associated with endosomal membranes of nonpolarized cells (34). Is it possible that like in the case of polarized exocytosis from the TGN (30), γ -adaptins also control exocytosis from endosomes in polarized cells? Ultrastructural observations revealed that in polarized MDCK cells, dIgA and hTfn are associated with basolateral endosomes whose tubules contain buds coated with γ -adaptin and clathrin lattices (15). Although this observation suggests that AP-1-containing clathrin coats in endosomes are involved in basolateral recycling, no direct evidence presently exists to support this hypothesis. If basolateral exocytosis and basolateral recycling share common sorting mechanisms, it is possible that during basolateral exocytosis, receptors targeted from the TGN to endosomes enter AP-1/clathrin-coated areas in endosomes (Fig. 9 *step 7*). In this scenario, endosomal AP-1 may mediate receptor exocytosis from endosomes as it is predicted to retrieve Tfn in endosomes into the basolateral recycling pathway (15). Basolateral recycling circuits in endosomes may hence be operational in exocytosis of membrane proteins to the basolateral cell surface.

Current data suggest that membrane recycling can take place via long and short recycling pathways. In polarized and nonpolarized cells, the bulk of recycling TfnRs is transported from early sorting endosomes to a juxtannuclear, pericentriolar, long-lived collection of tubulovesicular membranes (recycling endosomes) before returning to the plasma membrane (the long and slow circuit (66, 67)). The data also suggest that some receptors molecules can return from sorting early endosomes directly to the plasma membrane (the short and fast circuit (66, 68)). Not all receptors that reach recycling endosomes proceed from there to the plasma membrane. Some may be sorted back

FIG. 9. A model summarizing the possible exocytic and post-endocytic trafficking pathways taken by the pIgR in polarized MDCK cells. pIgR phosphorylated at Ser⁷²⁶ is marked with P. The model is based upon the meeting analysis performed in this study between biosynthetically labeled receptors and membrane-bound or fluid phase ligands internalized into apical or basolateral endosomes. Exocytic pathways are marked with solid arrows, whereas endocytic pathways are shown with dashed arrows.



to sorting early endosomes from where they can enter the direct recycling pathway (69). Any of these recycling circuits may be used by exocytic receptors (Fig. 9, steps 4, 6, 3, and 7). The hypothesis that early basolateral or apical endosomes are significant compartments for recycling of exocytic receptors is in agreement with recent findings suggesting that the majority of recycling in MDCK cells occurs from early endosomes, where little sorting of apical from basolateral proteins occurs (70). In any event, the fact that exocytic receptors traverse several endosomal compartments suggests that sorting and targeting during exocytosis is a multilayered process. Each endosomal compartment may serve as an intermediate checkpoint for inspection of receptor sorting and targeting to the next organelle, and this successive process may ensure receptor incorporation into the correct surface domain. The sequential role of rab GTPases (*e.g.* the early endosomal rab5a (71), the recycling endosome associated rab4 (72), and the ARE-CE bound rab11 and rab25 (14, 22)) along the endocytic and recycling pathway supports the idea that sorting and recycling endosomes are distinct compartments. Overexpression of rab proteins may hence provide a useful experimental system to study the identity and function of various endosomal compartments in polarized exocytosis of membrane proteins.

The exocytic and post-endocytic routes of basolateral recycling receptors almost completely avoid AEE but access apical endosomes loaded with a membrane-bound tracer (Fig. 9, steps 1 and 8). In contrast, the exocytic and post-endocytic pathways of transcytotic receptors access AEE (Fig. 9, step 5). This similar behavior suggests that at least in the case of the pIgR,

receptors traveling in the exocytic and post-endocytic routes are controlled by common endocytic compartments. Although this could be a satisfying and parsimonious model, it remains possible that in several cases exocytic and post-endocytic receptors occupy distinct endosomal subdomains. Consistent with this idea are results showing that mutations that impaired basolateral sorting of internalized hTfnRs did not affect basolateral sorting of the newly synthesized protein (73). Ultimately, more experimental studies are needed to further substantiate the relationship between endocytic compartments and polarized exocytosis from the TGN.

Acknowledgments—We thank G. Banting (University of Bristol, UK) for providing anti-TGN38 antibodies and K. Mostov (University of California, San Francisco, CA) for contributing anti-SC Fab fragments. We are grateful to Prof. Curtis Okamoto (University of Southern California, Los Angeles, CA), Prof. Jim Casanova (University of Virginia, Charlottesville, VA), Prof. Gerard Apodaca (University of Pittsburgh, Pittsburgh, PA), and Prof. Marshall Devor (The Hebrew University of Jerusalem) for many discussions and critical reading of the manuscript.

REFERENCES

- Keller, P., and Simons, K. (1997) *J. Cell Sci.* **110**, 3001–3009
- Aroeti, B., Okhrimenko, H., Reich, V., and Orzech, E. (1998) *Biochim. Biophys. Acta* **1376**, 57–90
- Matter, K., and Mellman, I. (1994) *Curr. Opin. Cell Biol.* **6**, 545–554
- Mostov, K., ter Beest, M. B. A., and Chapin, S. J., (1999) *Cell* **99**, 121–122
- Griffiths, G., and Simons, K. (1986) *Science* **234**, 4381–4443
- Rindler, M. J., Ivanov, I. E., Plesken, H., Rodriguez-Boulan, E., and Sabatini, D. D. (1984) *J. Cell Biol.* **98**, 1304–1319
- Fuller, S. D., Bravo, R., and Simons, K. (1985) *EMBO J.* **4**, 297–307
- Aroeti, B., and Mostov, K. E. (1994) *EMBO J.* **13**, 2297–2304
- Leitinger, B., Hille-Rehfeld, A., and Spiess, M. (1995) *Proc. Natl. Acad. Sci.* **92**, 10109–10113

10. Futter, C. E., Connolly, C. N., Cutler, D. F., and Hopkins, C. R. (1995) *J. Biol. Chem.* **270**, 10999–11003
11. Brachet, V., Pehau-Arnauudet, G., Desaymard, C., Raposo, G., and Amigorena, S. (1999) *Mol. Biol. Cell* **10**, 2891–2904
12. Mostov, K. E., Altschuler, Y., Chapin, S. J., Enrich, C. C., Low, S.-H., Luton, F., Richman-Eisenstat, J., Singer, K. L., Tang, K., and Weimbs, T. (1995) *Cold Spring Harbor Symp. Quant. Biol.* **LX**, 775–781
13. Gibson, A., Futter, C. E., Maxwell, S., Allchin, E. H., Shipman, M., Kraehenbuhl, J.-P., Domingo, D., Odorizzi, G., Trowbridge, I. S., and Hopkins, C. R. (1998) *J. Cell Biol.* **143**, 81–94
14. Brown, P. S., Wang, E., Aroeti, B., Chapin, S. J., Mostov, K. E., and Dunn, K. W. (2000) *Traffic* **1**, 124–140
15. Futter, C. E., Gibson, A., Allchin, E. H., Maxwell, S., Ruddock, L. J., Odorizzi, G., Domingo, D., Trowbridge, I. S., and Hopkins, C. R. (1998) *J. Cell Biol.* **141**, 611–623
16. Odorizzi, G., Pearse, A., Domingo, D., Trowbridge, I. S., and Hopkins, C. R. (1996) *J. Cell Biol.* **135**, 139–152
17. Knight, A., Hughson, E., Hopkins, C. R., and Cutler, D. F. (1995) *Mol. Biol. Cell* **6**, 597–610
18. Hughson, E. J., and Hopkins, C. R. (1990) *J. Cell Biol.* **110**, 337–348
19. Apodaca, G., Katz, L. A., and Mostov, K. E. (1994) *J. Cell Biol.* **125**, 67–86
20. Barroso, M., and Sztul, E. S. (1994) *J. Cell Biol.* **124**, 83–100
21. van Ijzendoorn, S. C., and Hoekstra, D. (1999) *Trends Cell Biol.* **9**, 144–149
22. Casanova, J. E., Wang, X., Kumar, R., Bhartur, S. G., Navarre, J., Woodrum, J. E., Altschuler, Y., Ray, G. S., and Goldenring, J. R. (1999) *Mol. Biol. Cell* **10**, 47–61
23. Apodaca, G., and Mostov, K. E. (1993) *J. Biol. Chem.* **268**, 23712–23719
24. Mostov, K. E., and Cardone, M. H. (1995) *Bioessays* **17**, 129–138
25. Song, W., Bomsel, M., Casanova, J., Vaerman, J.-P., and Mostov, K. E. (1994) *Proc. Natl. Acad. Sci. U. S. A.* **91**, 163–166
26. Hirt, R. P., Hughes, G. J., Frutiger, S., Michetti, P., Perregaux, C., Poulain-Godefroy, O., Jeanguenat, N., Neutra, M. R., and Kraehenbuhl, J.-P. (1993) *Cell* **74**, 245–255
27. Casanova, J. E., Breitfeld, P. P., Ross, S. A., and Mostov, K. E. (1990) *Science* **248**, 742–745
28. Casanova, J. E., Apodaca, G., and Mostov, K. E. (1991) *Cell* **66**, 65–75
29. Aroeti, B., Kosen, P. A., Kuntz, I. D., Cohen, F. E., and Mostov, K. E. (1993) *J. Cell Biol.* **123**, 1149–1160
30. Reich, V., Mostov, K., and Aroeti, B. (1996) *J. Cell Sci.* **109**, 2133–2139
31. Matter, K., Whitney, J. A., Yamamoto, E. M., and Mellman, I. (1993) *Cell* **74**, 1053–1064
32. Mauxion, F., Le Borgne, R., Munier-Lehmann, H., and Hoflack, B. (1996) *J. Biol. Chem.* **271**, 2171–2178
33. Honing, S., Sosa, M., Hille-Rehfeld, A., and von Figura, K. (1997) *J. Biol. Chem.* **272**, 19884–19890
34. Le Borgne, R., Griffiths, G., and Hoflack, B. (1996) *J. Biol. Chem.* **271**, 2162–2170
35. Le Borgne, R., and Hoflack, B. (1997) *J. Cell Biol.* **137**, 335–345
36. Hunziker, W., and Geuze, H. (1996) *Bioessays* **18**, 379–389
37. Orzech, E., Schlessinger, K., Weiss, A., Okamoto, C. T., and Aroeti, B. (1999) *J. Biol. Chem.* **274**, 2201–2215
38. Podbilewicz, B., and Mellman, I. (1990) *EMBO J.* **9**, 3477–3487
39. Wilde, A., Reaves, B., and Banting, G. (1992) *FEBS Lett.* **313**, 235–238
40. Breitfeld, P., Casanova, J. E., Harris, J. M., Simister, N. E., and Mostov, K. E. (1989) *Methods Cell Biol.* **32**, 329–337
41. Brewer, C. B. (1994) *Methods Cell Biol.* **43**, 233–245
42. Breitfeld, P. P., Casanova, J. E., McKinnon, W. C., and Mostov, K. E. (1990) *J. Biol. Chem.* **265**, 13750–13757
43. Courtoy, P. J., Quintart, J., and Baudhuin, P. (1984) *J. Cell Biol.* **98**, 870–876
44. Geuze, H. J., Stoorvogel, W., Strous, G. J., Slot, J. W., Bleekemolen, J. E., and Mellman, I. (1988) *J. Cell Biol.* **107**, 2491–2501
45. White, S., Miller, K., Hopkins, C., and Trowbridge, I. S. (1992) *Biochim. Biophys. Acta* **1136**, 28–34
46. Anderson, J. M., Stevenson, B. R., Jesatis, L. A., Goodenough, D. A., and Mooseker, M. A. (1988) *J. Cell Biol.* **106**, 1141–1149
47. Castel, M., Belenky, M., Cohen, S., Ottersen, P. O., and Storm-Mathisen, J. (1993) *Eur. J. Neurol.* **5**, 368–381
48. Bomsel, M., Prydz, K., Parton, R. G., Gruenberg, J., and Simons, K. (1989) *J. Cell Biol.* **109**, 3243–3258
49. Parton, R. G., Prydz, K., Bomsel, M., Simons, K., and Griffiths, G. (1989) *J. Cell Biology* **109**, 3259–3272
50. Balin, B. J., and Broadwell, R. D. (1988) *J. Neurocytol.* **17**, 809–826
51. Raub, T. J., Koroly, M. J., and Roberts, R. M. (1990) *J. Cell. Physiol.* **144**, 52–61
52. Raub, T. J., Koroly, M. J., and Roberts, R. M. (1990) *J. Cell. Physiol.* **143**, 1–12
53. Chavrier, P., Parton, R. G., Hauri, H. P., Simons, K., and Zerial, M. (1990) *Cell* **62**, 317–329
54. Apodaca, G., Aroeti, B., Tang, K., and Mostov, K. E. (1993) *J. Biol. Chem.* **268**, 20380–20385
55. Folsch, H., Ohno, H., Bonifacino, J. S., and Mellman, I. (1999) *Cell* **99**, 189–198
56. Low, S. H., Tang, B. L., Wong, S. H., and Hong, W. (1992) *J. Cell Biol.* **118**, 51–62
57. Johnson, K. F., and Kornfeld, S. (1992) *J. Cell Biol.* **119**, 249–257
58. Dittie, A. S., Thomas, L., Thomas, G., and Tooze, S. (1997) *EMBO J.* **16**, 4859–4870
59. Wan, L., Molloy, S. S., Thomas, L., Liu, G., Xiang, Y., Rybak, S. L., and Thomas, G. (1998) *Cell* **94**, 205–216
60. Ikonen, E., Tagaya, M., Ullrich, O., Montecucco, C., and Simons, K. (1995) *Cell* **81**, 571–580
61. Apodaca, G., Cardone, M. H., Whiteheart, S. W., DasGupta, B. R., and Mostov, K. E. (1996) *EMBO J.* **15**, 1471–1481
62. Boll, W., Partin, J. S., Katz, A. I., Caplan, M. J., and Jamieson, J. D. (1991) *Proc. Natl. Acad. Sci. U. S. A.* **88**, 8592–8596
63. Cowles, C. R., Odorizzi, G., Payne, G. S., and Emr, S. D. (1997) *Cell* **91**, 109–118
64. Menon, A. (1998) *Trends Cell Biol.* **8**, 374–376
65. Robinson, M. (1990) *J. Cell Biol.* **111**, 2319–2326
66. Hopkins, C. R., Gibson, A., Shipman, M., Strickland, D. K., and Trowbridge, I. S. (1994) *J. Cell Biol.* **125**, 1265–1274
67. Marsh, E. W., Leopold, P. L., Jones, N. L., and Maxfield, F. R. (1995) *J. Cell Biol.* **129**, 1509–1522
68. Daro, E., van der Sluijs, P., Galli, T., and Mellman, I. (1996) *Proc. Natl. Acad. Sci. U. S. A.* **93**, 9559–9564
69. Ghosh, R. N., and Maxfield, F. R. (1995) *J. Cell Biol.* **128**, 549–561
70. Sheff, D. R., Daro, E. A., Hull, M., and Mellman, I. (1999) *J. Cell Biol.* **145**, 123–139
71. Bucci, C., Wandinger-Ness, A., Lutcke, A., Chiariello, M., Bruni, C. B., and Zerial, M. (1994) *Proc. Natl. Acad. Sci. U. S. A.* **91**, 5061–5065
72. van der Sluijs, P., Hull, M., Webster, P., Male, P., Goud, B., and Mellman, I. (1992) *Cell* **70**, 729–740
73. Odorizzi, G., and Trowbridge, I. S. (1997) *J. Cell Biol.* **137**, 1255–1264
74. Distel, B., Bauer, U., Le Borgne, R., and Hoflack, B. (1998) *J. Biol. Chem.* **273**, 186–193
75. Reaves, B., and Banting, G. (1994) *FEBS Lett.* **351**, 448–456